BIODIVERSITAS
Volume 23, Number 4, April 2022
Pages: 2066-2079

ISSN: 1412-033X
E-ISSN: 2085-4722
DOI: 10.13057/biodiv/d230442

Morphological and molecular characterization of *Distichochlamys citrea* M.F. Newman in Bach Ma National Park, Thua Thien Hue Province, Vietnam

TRAN VAN CHEN[1], NGUYEN DUC TUAN[2], NGUYEN THANH TRIET[3,♥], NGUYEN HOANG AN[2], PHAN THI THAO NGUYEN[2,6], NGUYEN THI THANH HAI[4], NGUYEN THANH TO NHI[5], NGUYEN QUANG CO[6], HO THI HOANG NHI[6], HOANG VIET HUONG[7], TRUONG THI BICH PHUONG[2,♥♥], NGUYEN THI AI NHUNG[4]

[1]Faculty of Pharmacy, University of Medicine and Pharmacy. Ho Chi Minh City 700000, Vietnam
[2]Department of Biology, University of Sciences, Hue University. Hue City 530000, Vietnam. ♥♥email: ttbphuong@hueuni.edu.vn
[3]Faculty of Traditional Medicine, University of Medicine and Pharmacy. Ho Chi Minh City, 700000, Vietnam. ♥email: nguyenthanhtriet1702@ump.edu.vn
[4]Department of Chemistry, University of Sciences, Hue University. Hue City 530000, Vietnam
[5]Faculty of Pharmacy, Nguyen Tat Thanh University. Ho Chi Minh City 700000, Vietnam
[6]Institute of Biotechnology, Hue University. Hue City 530000, Vietnam
[7]Department of Science and Technology, Thua Thien Hue Province, Vietnam

Manuscript received: 18 February 2022. Revision accepted: 25 March 2022.

Abstract. *Chen TV, Tuan ND, Triet NT, An NH, Nguyen PTT, Hai NTT, Nhi NTT, Co NQ, Nhi HTH, Huong HV, Phuong TTB, Nhung NTA. 2022. Morphological and molecular characterization of* Distichochlamys citrea *M.F. Newman in Bach Ma National Park, Thua Thien Hue Province, Vietnam. Biodiversitas 23: 2066-2079. Distichochlamys citrea* (Black Ginger or gung den) is a medicinal plant endemic to Vietnam. However, this species is not easily identified due to the lack of a detailed description. Therefore, this study aimed to characterize morphological and molecular aspects of *D. citrea* from Bach Ma National Park, Vietnam. Six representative plants were selected for the following analyses. Macromorphological features were observed and compared with previous studies. The rhizomes, roots, petioles, and leaves were then histologically analyzed using iodine green-carmine staining. The ground rhizomes and leaves were also microscopically examined for powder characteristics. Finally, the *D. citrea* DNA barcode was amplified by Internal Transcribe Spacer (ITS) primers. Macromorphologically, *D. citrea* differs from other *Distichochlamys* species. Black Ginger, particularly, has elongated rhizomes (with scars from the shoots of previous years), green leaves, spread inflorescences, and yellow labellum (with deep slits). Additionally, *D. citrea*'s micromorphological structures (epidermis, exodermis, hypodermis, cortex, endodermis, and root pith) are similar to the genus *Zingiber*. However, the absence of calcium oxalate and silica crystals in the root is unique and can be used to distinguish this plant from other Zingiberaceae members. The sequenced amplicons (96.54% similar to Genbank's *D. citrea* ITS) demonstrated the ITS marker's ability to identify Black Ginger.

Keywords: *Distichochlamys citrea*, ITS, macromorphological features, micromorphological structures, powder characteristics

Abbreviations: ddw: double distilled water; ITS: Internal Transcribe Spacer; PCR: Polymerase Chain Reaction

INTRODUCTION

Distichochlamys (Zingiberaceae) is a plant genus endemic to Vietnam, with four discovered species. *D. citrea*, also known as Black Ginger or gung den, is the first *Distichochlamys* species found in Bach Ma National Park, Thua Thien Hue Province, Vietnam (Newman 1995; Nguyen and Leong-Škorničková 2012). The appearance of *D. citrea* has also been reported in other regions of Vietnam, including Quang Binh, Quang Tri, Quang Nam, and Nghe An province (Huong et al. 2017; Ty et al. 2017). After the discovery of *D. citrea*, three other species of the genus *Distichochlamys* were also found at different Vietnamese locations, including *D. orlowii* K. Larsen & M.F.Newman (Gia Lai Province) (Larsen and Newman 2001), *D. rubrostriata* W.J.Kress & Rehse (Cuc Phuong National Park) (Rehse and Kress 2003), and *D. benenica* Q.B.Nguyen & Škorničk (Thanh Hoa Province and Ben En National Park) (Rehse and Kress 2003; Nguyen and Leong-Škorničková 2012).

Huong et al. (2017) and Hoang et al. (2020) reported the chemical compositions of *D. citrea* essential oil (extracted from rhizomes), namely 1,8-cineol, citral A, citral B, geraniol, geranyl acetate, terpinen-4-ol, linalool, borneol, and α-terpineol. The mentioned substances have important health benefits, such as anticancer, anti-inflammatory, antibacterial, antiplasmodial, antihyperalgesic, enhancing drug permeability, antioxidant, anticonvulsant, and antiulcer activities (Moteki et al. 2002; Carnesecchi et al. 2004; Kamatou and Viljoen 2008; Quintans-Júnior et al. 2011; Khaleel et al. 2018). In addition, *D. citrea* has long been used as a medicine for infecting diseases and a spice by Vietnamese ethnic groups, including the Pakô people (Huong et al. 2017).

Detailed descriptions of both macro-and micromorphological features of the genus *Distichochlamys* (including *D. citrea*) have never been reported. Thus, the anatomical identification *D. citrea* becomes extremely confusing. To our knowledge, there are four studies on *Distichochlamys* spp. morphological features, including Newman (1995), Larsen and Newman (2001), Rehse and Kress (2003), and Nguyen and Leong-Škorničková (2012). However, all of these studies focused only on macromorphological characteristics for plant classification. No study on micromorphological for plant identification and standardization of raw materials has been reported so far. Therefore, this is the first research presenting both macro-and micromorphological characteristics of *D. citrea* to serve as a premise for further studies on this herb.

DNA barcoding is an effective and reliable tool that can be used to support traditional taxonomy based on morphological features (Hebert et al. 2003; Packer et al. 2009; Li et al. 2011). Additionally, DNA barcoding was also used to identify medicinal plants (Techen et al. 2014). Of all the DNA barcodes, ITS has been reported to have more discriminating power than plastid regions at low taxonomic levels (Hollingsworth et al. 2011). Moreover, huge numbers of plant species were successfully identified by using ITS (Kress and Erickson 2007; Gonzalez et al. 2009; Chen et al. 2010; Yao et al. 2010). To date, ITS regions of *D. citrea* have been deposited on Genbank by several authors, such as (Kress et al. 2002; Ngamriabsakul et al. 2003; Sam et al. 2016) facilitating the ITS-based identification of black ginger.

Considering the lack of scientific evidence for identifying *D. citrea* and the competence of ITS DNA barcodes, this study aimed to characterize macro-and micromorphological features and sequence the ITS region to provide detailed and precise information about this species. The results of our study set the standard for *D. citrea* identification to distinguish this plant from other species and select the correct species for medicinal uses.

MATERIALS AND METHODS

Plant materials

Distichochlamys citrea fresh plants were collected from Bach Ma National Park (Thua Thien Hue, Vietnam), where this species is mainly found. Six samples were collected from several locations in the National Park. The plants were then washed and air-dried for macro-and micromorphological analyses. Several fresh leaves were also cut and stored in sealed plastic bags at 4°C for DNA extraction.

Procedures of morphological study

Macromorphological characteristics

The macromorphological features of rhizome, root, petiole, leaf, and inflorescence of *D. citrea* were compared with the taxonomy key, pictures, and descriptions in the references, such as (Newman 1995; Larsen and Newman 2001; Rehse and Kress 2003; Nguyen and Leong-Škorničková 2012).

Micromorphological characteristics

The micromorphological features of rhizomes, roots, leaves, and petioles were determined by using the iodine green-carmine double staining method of Vietnam Pharmacopoeia V (Ministry of Health 2017). First, the roots and rhizomes were cut into pieces (about 1.0 to 3.0 cm long). The leaves (including the main veins) were also cut into segments (about 1.0 cm wide and 2.0 to 3.0 cm long). Then, the specimens were sliced into thin pieces using a razor blade. Next, the representative samples were chosen for staining. The selected slices were macerated and made clear with 5% (w/v) chloramine-T. After that, the samples were immersed in 50% (v/v) chloral hydrate reagent for 10 minutes before being acidified with 1% (w/v) acetic acid for two minutes. The processed slices were stained with 0.3% (w/v) Iodine Green (one to five seconds) and 1% (w/v) Carmine (until the color of the slices became obvious). The excess reagents (chloramine-T, chloral hydrate, acetic acid, Iodine Green, and Carmine) were removed after each step by double-distilled water (ddw). The stained specimens were covered by coverslips and observed under a microscope (HumaScope, Germany).

In the leaf epidermis analysis, two to three fresh leaves were taken and torn directly using tweezers (Li et al. 2019). The steps were as follows (Zahara (2019). Firstly, the upper and the lower surfaces of the leaves were washed and the epidermises of both surfaces were peeled off. The cuticle pieces were placed on glass slides with a drop of water. The specimens were covered by coverslips and their stomata patterns were observed under a microscope (HumaScope, Germany) with magnifications of 10X and 40X.

The features of the rhizome and leaf powders were determined by using the protocol described by Vietnam Pharmacopoeia V (Ministry of Health 2017). The leaf and rhizome powders were first passed through a sieve (mesh size: 250 µm) to remove coarse particles. A small amount of powder was placed on a glass slide and mixed with a drop of water, using a needle. The specimens were covered by coverslips and observed under a microscope (HumaScope, Germany).

Procedures of molecular study

DNA extraction and Polymerase Chain Reaction (PCR)

Total genomic DNA extraction was done by using the protocol of Khanuja et al. (1999). The concentrations of DNA solutions were determined by the Gene Quant spectrophotometer at the wavelengths of 260, 280, and 230 nm. The DNA solutions were then stored at -20 °C (Khanuja et al. 1999).

The ITS sequence of five DNA samples was amplified by using the ITS1 and ITS4 primers (5'-3' sequences: TCCGTAGGTGAACCTGCGG and TCCTCCGCTTATTGATATGC, respectively) (Cheng et al. 2016). PCRs were performed in a volume of 25 µL and contained 1.25 µL of ITS1 primer (10 µM), 1.25 µL of ITS4 primer (10 µM), 12.5 µL of 2X GoTaq Green Master Mix (Promega, USA), 0.5 µL of the extracted DNA solution (25 µg/µL), and 9.5 µL of nuclease-free ddw. The reactions were placed in the Mastercycler device

(Eppendorf, Germany). PCR steps were as follows: initial denaturation at 94ºC for 3 minutes, 35 amplification cycles (denaturation at 94ºC for 1 minute, annealing at 54ºC for 1 minute and primer extension at 72ºC for 2 minutes), and final extension at 72ºC for 10 minutes.

The electrophoresis of the PCR product was done on a 0.6% agarose gel. GeneRuler Express DNA Ladder (Thermo Fisher Scientific, #SM1553, 100 - 5000 bp) was used to determine the amplicon's length.

Purification and DNA sequencing

The PCR product was purified and sequenced by Nam Khoa BioTek Company (Vietnam). The Sanger sequencing was done by using a 3130xl Genetic Analyzer (16-capillary array). After that, regions containing weak or noisy signals in the raw sequence were removed.

Data analysis

Macromorphological features

Six samples were randomly collected from different locations in Bach Ma National Park. Before sample collection, the shape, color, and aroma of the herbs were recorded. Additionally, the heights, lengths, and widths of the aerial shoots, leaves, petioles, inflorescences, and bracts were measured using a standard ruler (smallest unit: 1mm). The herbs were then dug up, and their rhizome circumferences were measured. The color and the growth direction of the main rhizome were also recorded. All the measured parameters of the plants were used to calculate means and standard deviations by using Microsoft Excel 2016. The maximum and minimum values were also shown along with the means.

Micromorphological features

The six collected representative samples were used for micromorphological and powder analyses. Cell size and cell components were measured by eyepiece micrometers (Olympus, Japan), according to the guidelines of Vietnam Pharmacopoeia V (Ministry of Health 2017). Measurements were done under high magnifications (10X, 40X). However, for measuring large structures (including fibers and hairs), small magnifications (4X, 10X) were used. All the measured values (length, width/diameter, number of cell layers, number of vascular bundles) were shown as mean ± SD (Standard Deviation), maximum, and minimum values (μm). The calculations were done by using Microsoft Excel 2016.

ITS analysis

DNA sequencing accuracy examination and consensus sequence construction were done by Seaview and Mega11 software packages. After the sequence examination, three in five sequences were eliminated due to the high proportion of noisy signals. The remaining sequenced PCR products were used as the query for BLAST (Basic Local Alignment Search Tool) in the genus *Distichochlamys* (taxid: 97740) to identify the species name. Then, our amplicon (MZ310840) was compared with four ITS sequences of *D. citrea* (accession numbers: AF478744, AY424757, AJ388282, and AB552946), one ITS sequences of *D. rubrostriata* (HM236130), and nine random ITS sequences of different species in the Zingiberaceae family (AF478788, LC148074, LC148080, KY492399, HM236152, LC148062, AB245522, KY492426, and KY701326) by using a dendrogram (maximum likelihood, bootstrap = 1000) to confirm the efficiency of ITS in *D. citrea* identification (Table 1). The dendrogram was constructed by the Mega11 software.

RESULTS AND DISCUSSION

Morphological characters

Macromorphological features

Distichochlamys citrea is a species in the ginger family, so it generally bears a high similarity to other species of the family Zingiberaceae. However, this species also carries features that are specific to the genus and the species. The species description of *D. citrea* is as follows:

The habit of *D. citrea* is a small rhizomatous herb, composed of the aerial shoot (leafy shoots), underground parts (rhizomes, roots), and leaves (petioles, leaf blades) (Figure 1).

Aerial shoot and rhizome: the aerial shoot is about 38-48 cm (42.75 ± 4.09 cm) high (Figure1a) and made of 1-3 leaves, densely clustering with other shoots. The basal sheaths of shoots are up to 10 cm, reddish, and turned brown when they dried. The rhizome is long, cylindrical, and light-yellow, with nodes and scars of aerial shoots from former years. The cross-sectional surface of the rhizome is yellow-white or pale yellow and has a circle (Figure 1e). The fibers of the rhizome are yellow-white (Figure 1f). The rhizome has a unique aroma and mildly spicy taste. The rhizome has many adventitious roots, 5 - 23 cm (-30) cm (19.5 ± 10.13 cm) in length and 0.5-1.0 cm (0.9 ± 0.26 cm) in diameter (Figure 1g).

Leaves: the mature petiole is 20 cm high. The base part of the petiole is red-violet, which gradually fades to translucent green towards the leaf blade. The elliptical leaf blades have a length of 18-22 cm (19.92 ± 1.43 cm) and a width of 8.0-10.7 cm (9.5 ± 1.08 cm). The shortleaf tip is sail-shaped or round. The lower sides of leaf blades are light green and nearly parallel to the rhizome, while their upper sides are smooth and dark green. The midribs of leaf blades are obvious (Figure 1a).

Inflorescence: inflorescences grow close to the ground from the rhizome and consist of one or two flowers. It is 9.5-10 cm (9.6 ± 0.28 cm) high. The spread bracts are 2.5-3.2 cm (2.92 ± 0.28 cm) long, tubular, and dark reddish-pink. The bracteoles, having intact edges, are 1.9-2.5 cm (2.22 ± 0.23 cm) long, tubular, and reddish-brown (Figure1c).

Flowers: petals are yellow, spoon-shaped, and slightly curved backward. Petals have three stripes extending from the base to the tip. Calyx and corolla tubes are 1.2-1.5 cm long and contain four lobes, including two wide anterior corolla lobes and two narrow dorsal corolla lobes. The clefts of the labella extend to their center (Figure1d).

Table 1. The sequences used in constructing the maximum likelihood dendrogram

Species names	Accession numbers	References
Distichochlamys citrea	MZ310840	Our sequence
Distichochlamys citrea	AF478744	Kress et al. (2002)
Distichochlamys citrea	AY424757	Ngamriabsakul et al. (2003)
Distichochlamys citrea	AJ388282	Searle and Hedderson (2000)
Distichochlamys rubrostriata	HM236130	Zheng and Xia (2010)
Distichochlamys citrea	AB552946	Sam et al. (2016)
Scaphochlamys biloba	AF478788	Kress et al. (2002)
Scaphochlamys perakensis	LC148074	Sam et al. (2016)
Scaphochlamys endauensis	LC148080	Sam et al. (2016)
Borneocola calcicola	KY492399	Ooi (2018)
Zingiber ellipticum	HM236152	Zheng and Xia (2010)
Borneocola calcicola	LC148062	Sam et al. (2016)
Myxochlamys mullerensis	AB245522	Takano and Nagamasu (2007)
Scaphochlamys malaccana	KY492426	Ooi (2018)
Boesenbergia bella	KY701326	Mood et al. (2019)

Macromorphological characteristics of *D. citrea* in Bach Ma National Park are similar to those described by Newman (1995). However, it is not reliable to identify a plant species based on macromorphological features since they can be affected by environmental factors (Szczepaniak et al. 2002; Conklin et al. 2009; Uma and Muthukumar 2014). The species could be distinguished from other species by flower and leaf characteristics and colors, inflorescence, and leaf color, based on the *Distichochlamys* taxonomy key of Newman (1995), Larsen and Newman (2001), Rehse and Kress (2003), and Nguyen and Leong-Škorničková (2012). Specifically, the leaf sheath of *D. citrea* is longer than that of other species (9.0-10 cm). Black ginger's lower surface of the leaves is light green and smooth, while the ones of *D. orlowii* and *D. benenica* are dark red and light green with a purple tint at the base, respectively. The upper surface of *D. citrea* leaves has a glossy dark green color, while the ones of the other species are only dark green. The inflorescence of *D. citrea* has spread bracts, while the other species have the bracts, which are firmly attached. The labellum of *D. citrea* flower has a cleft being as long as half of its length, whereas the other species have clefts, extending less than half of their length. The detailed features are shown in Table 2.

Micromorphological features

Leaves

The horizontally cut surface of the *D. citrea* leaf is axially symmetric. The upper surface of the leaf formed a pointed concave, while its lower surface is a round convex. The structure of the leaf included the following parts:

Midrib and vascular bundles

The upper and lower epidermises possess a thin cuticle covering the outer cell wall (Figures 2a and 2i). The hypodermis of the midrib consisting of parenchyma cells, is 2-3 layers thick (Figure 2b). The midrib tissue contains irregularly-sized collenchymatous cells (46-62 μm long and 50-63 μm wide), which form 7-8 cell layers (Figure 2d). The vascular bundles have xylems (94-345 μm in vertical diameter) being above phloems (Figures 2f and 2g). The bundles are covered by a ring of the irregularly-sized sclerenchymatous sheath. The vascular bundle sheath has three to six layers of sclerenchyma cells (35-38 μm long) (Figure 2h). All vascular bundles are lined up above the leaf's lower epidermis. The largest vascular bundle is located in the middle vein, being close to the leaf's lower epidermis. The sizes of vascular bundles gradually become smaller towards the left and the right sides of the leaf blades (Figures 2A and 2C). The parenchyma tissue (Figure 2d) contains small cells, a large air cavity (90-125 μm in vertical diameter and 94-107 μm in horizontal diameter) (Figure 2e), and many chloroplasts (Figure 2c), interlaced between the phloem-xylem bundles (Figure 2A, B, C). In the center of the midrib, there is a 78-95 μm long vascular bundle of phloem and xylem (young leaves) or 3-4 randomly organized vascular bundles (old leaves), which sometimes contain phloem being above xylem (Figure 2A).

Leaf blade

In the transverse section, the upper and lower epidermises are composed of polygonal cells. Cells in the upper epidermis (Figure 2a) are larger than in the lower epidermis (Figure 2i). Both the epidermises have stomata (j), with a presence in the lower epidermis more than the upper one. The stomata are paracytic, with rectangular subsidiary cells (17 μm long and 25 μm wide). There is one layer of non-continuous hypodermis cells (Figure 2b) (below the epidermises). The leaf blade consists of 4-5 layers of collenchymatous cells. The middle cells contain many chloroplasts (Figure 2c).

Stomata

The stomata are paracytic, with epidermal cells (10-12.5 μm long and 15-19 μm wide) (Figure 3B-b) being parallel to the opening between the guard cells (21-24 x 16-20 μm in diameter) (Figure 3B-a). The stomata are found on both sides of the leaves.

Petiole

The transverse section of the petiole is nearly oval-shaped, with a deep concave on the upper surface. The petiole consists of an epidermis (20-22 μm long (21.25 ± 0.37 μm)) (Figure 4a), hypodermis (Figure 4b), phloem-

xylem bundles (Figures 4h and 4g) and its structure is almost similar to that of the leaf. The uneven-sized phloem-xylem bundles form 2-3 arc-shaped rows. The randomly arranged upper row is in the middle of the petiole and contains phloem-xylem bundles. The other two rows consist of vascular bundles, which are evenly lined up. The largest vascular bundles are found in the middle row, containing xylems (Figure 4g) being above phloem (Figure 4h). These large bundles are interlaced by air cavities (93-125 µm (112.46 ± 0.24 µm) in vertical diameter and 120-125 µm (122.47 ± 0.24 µm) in horizontal diameter) (Figure 4c). The parenchyma (Figure 4f), surrounding these bundles, contains many chloroplasts (Figure 4e). There are also rings of the sclerenchymatous sheaths outside the bundles (22-40 µm long (31.2 ± 0.49 µm)) (Figure 4d).

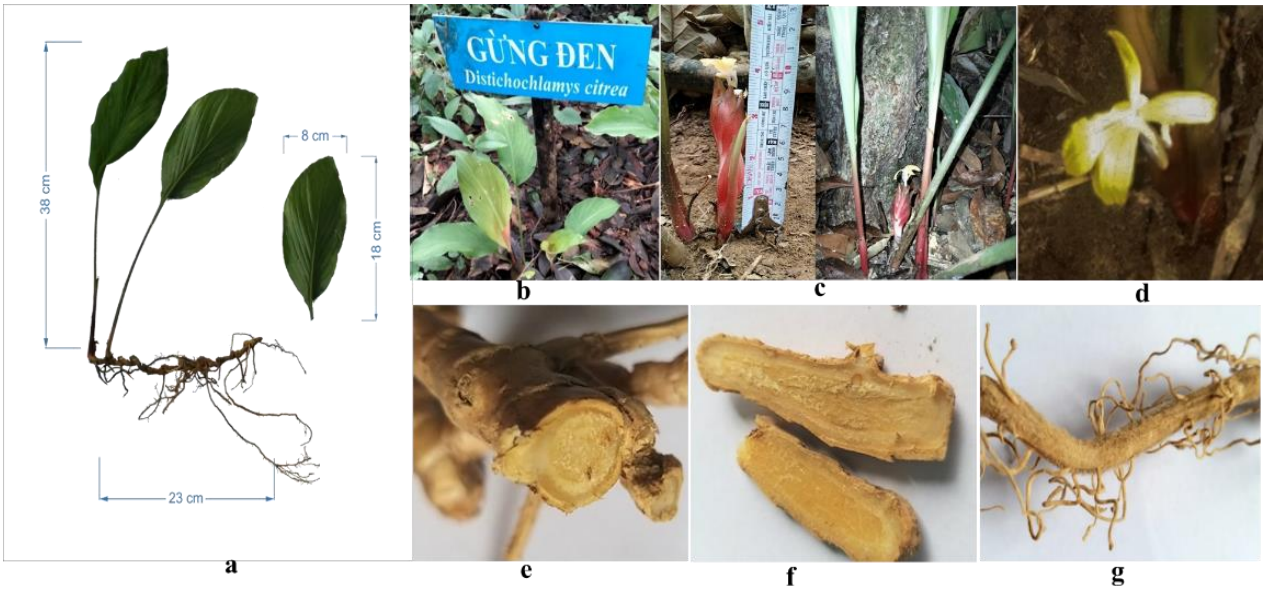

Figure 1. Morphological features of *D. citrea* from Bach Ma National Park: (a) all parts of the plants; (b) habit (herb); (c) inflorescence; (d) flower; (e, f) cross-sections of the rhizomes; (g) root and root hairs after drying

Table 2. Morphological characters comparison of *D. citrea* and other species within genus *Distichochlamys*

Morphological characteristics	***D. citrea* (The result of the present study and Newman 1995)**	***D. orlowii* (Larsen and Newman 2001)**	***D. rubrostriata* (Rehse and Kress 2003)**	***D. benenica* (Nguyen and Leong-Škorničková 2012)**
Habitus	Small herb to 38-48cm	Acaulescent, rhizomatous herb	Small evergreen herb to 30 cm	Terrestrial rhizomatous herb to 60 cm
Leaf sheath	9.0-10 cm long	4.0-7.0 cm long	6.0 cm long	3.0-5.0 cm long
Petiole	20-25 cm long, red-violet (at base), green (at apex)	15-20 cm long, green	8.0-25 cm long, maroon red-pigmented (at base), green (at apex), has scattered white spots	14-23 cm long, dark red-purple
Leaf blade	18-22 x 8-10.7 cm	15-27 x 8.5-13 cm	18-20 x 9.0-12 cm	15-28 × 10-14.5 cm
The lower surface of leaf	Smooth, light green	Dark red-purple	Light green	Light green with purple shaded at the beneath of the apex
The upper surface of leaf	Glossy, dark green	Dark green	Dark green	Dark green
Inflorescence	9.5-10 cm long	6.0-10 cm long	9.5-11.5 cm long	15 cm long
Peduncle	1.5-2.5 cm	1.0 cm	4.0-6.0 cm	3.0-6.0 cm
Bracts	Spread bracts, loosely imbricated, dark pinky-red	Bracts appressed to the floral axis, densely imbricated, green with red margins	Bracts appressed to the floral axis, densely imbricated, light green with maroon pigmented dot clusters	Bracts appressed to the floral axis, densely imbricated, more or less pink-red tinge
Flower	1-2	2-3	2-3	2-3
Labellum	Yellow, with deep cleft (extending to half of the labellum length), undivided lobes	Divided labellum with cleft (extending less than half of the labellum length), yellow, with purple veins, having dark yellow band and two emarginate lobes	Divided labellum (with cleft extending less than half of its length); yellow with two linear red patches at the base	Divided labellum (with cleft extending less than half of its length); yellow, with a red patch at base and two round lobes at the apex

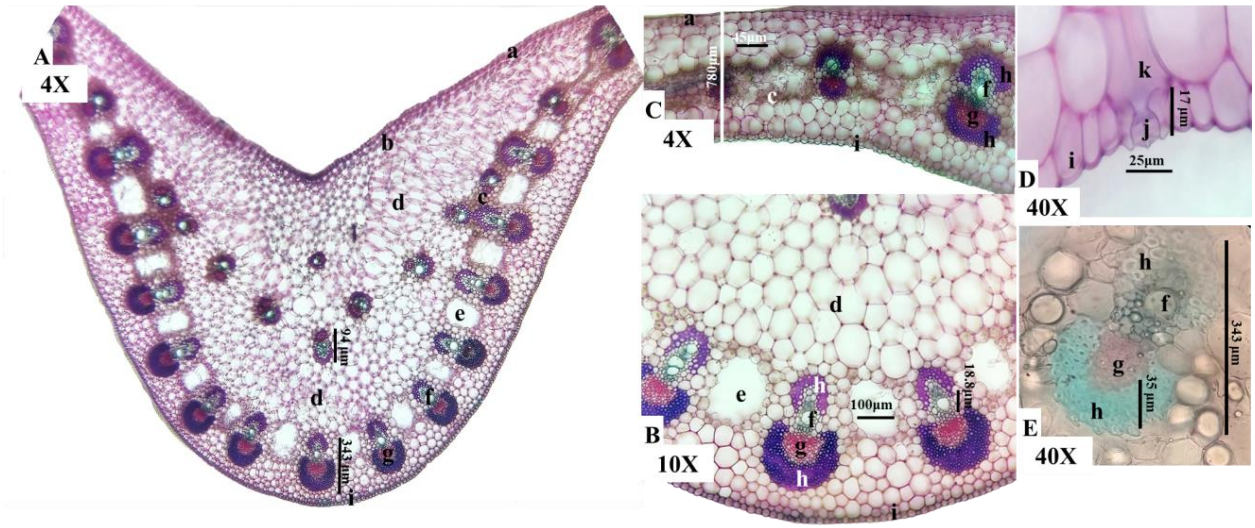

Figure 2. The features of the *D. citrea*'s cross-sectioned leaves (4X, 10X, 40X): (A, B) midrib, (C) leaf blade, (D) stomata, (E) vascular bundles. (a) upper epidermis; (b) hypodermis; (c) Chloroplasts; (d) collenchymatous cell/ parenchyma tissue; (e) air cavity; (f) xylem; (g) phloem; (h) sclerenchymatous bundle sheath; (i) lower epidermis; (j) stomata; (k) sub-stomatal cavity.

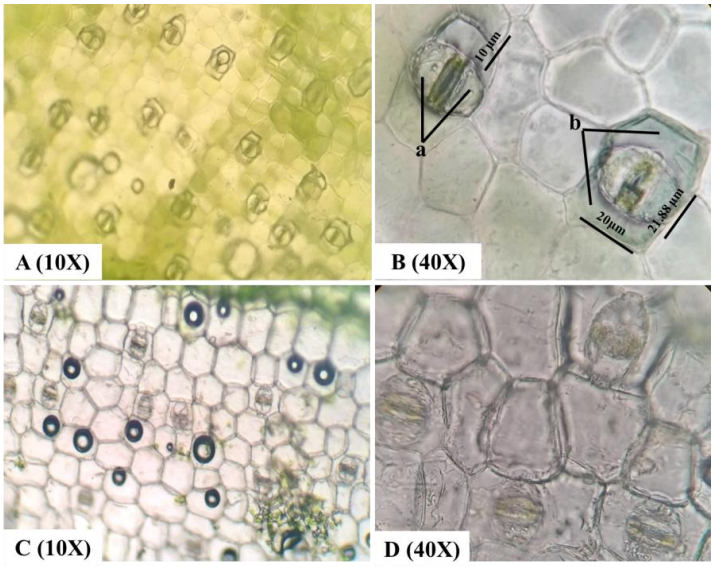

Figure 3. Epidermis with stomata of *D. citrea*: (A, B) surface view of the lower epidermis; (C, D) surface view of the upper epidermis; (a) guard cells; (b) epidermal cells.

The paracytic typed stomata, mesophyll cells, and vascular bundles in the leaf of *D. citrea* are similar to *Zingiber officinale* Roscoe (Rudall et al. 2017; Zahara 2019). However, silica cells (present in *Z. officinale* leaves) were not found in the leaves of *D. citrea* (Liu et al. 2020). Silicon (Si) is found in high levels (up to 10%) in monocotyledonous plants (especially grasses). In plant tissues, Si is commonly found as hydrogen bound Si-organic complexes and permeates epidermal and vascular walls, with the roles of strengthening plant tissues and reducing transpiration and fungal infections (Greger et al. 2018). The beneficial roles of Si in plant physiology (including regulation of defense-related enzymes, plant hormone signaling, and alteration of volatile plant compounds) make clear the association of Si with biochemical/molecular defense mechanisms. Like the above-ground parts of plants, the lower parts of plants also face threats from root-eating insects. Attacks on shoots by insects can also lead to root protective responses against root-eating species (Alhousari and Greger 2018).

Phylogenetic studies suggest that differences in the appearances, densities, and locations of proteins involved in Si transport are responsible for distinct plant abilities' of Si accumulations (Yan et al. 2018). Therefore, the absence of silica cells in the leaves of *D. citrea* compared to other species (in the Zingiberaceae family) might be a unique feature for this species in terms of Si transporting proteins.

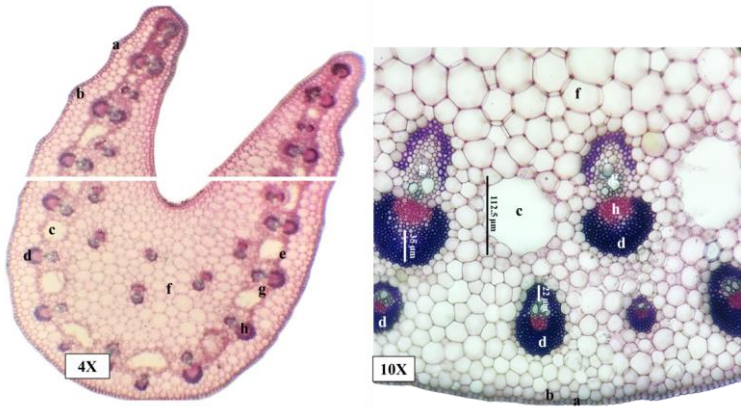

Figure 4. The features of the *D. citrea*'s cross-sectioned petiole: (a) epidermis; (b) hypodermis; (c) air cavity; (d) sclerenchymatous bundle sheath; (e) chloroplasts; (f) parenchyma; (g) xylem; (h) phloem.

Root and rhizome

Root

The transverse section of a root is nearly round and includes two distinct areas (the cortex zone and the pith). The cortex zone positioned below the root hair-bearing exodermis (Figure 5a) occupies about 2/3 of the section radius (370-380 µm wide). The suberized hypodermal cells consist of 3-5 layers of rectangular or polygonal cells (60-65 µm wide), which have thick cell walls and are arranged close together (Figure 5b). The intercellular spaces among the parenchymatous cells in the outer cortex (which are polygonal and randomly arranged) are small (Figure 5d). The parenchymatous tissue of the inner cortex has 4-5 layers of oval cells and is arranged into concentric rings and radial lines (90-95 µm wide) (Figure 5d). Many oil cells are scattered in the cortex tissue (Figure 5c). The U-shaped and continuous endodermis have thick-walled cells (5.5-6.5 µm long) (Figure 5e). The pith accounts for 1/3 of the root section radius. The pericycle, an irregularly sized polygonal cell layer, tends to be pressed flat above the xylem poles (Figure 5f). The vascular cylinder has more than 15 arches with scalariform perforation plates. The vascular bundles are located in the sclerenchyma. The rings created by interlacing the phloem and xylem, are below the pericycle. Each xylem bundle (consisting of 1-2 protoxylems (Figure 5h) and many large irregularly sized metaxylems (24.5-25.5 µm in horizontal diameter)) (Figure 5i) is arranged around the stele. The stele contains polygonal thick-walled cells (340-348 µm in horizontal diameter). The sclerenchyma gradually disappears towards the stele region (Figure 5j). The parenchymatous pith is in the middle of the stele (94-113 µm wide) (Figure 5k). Lateral roots originate from the pericycle of the stele region (Figure 5m).

Rhizome

The structure of the rhizome is almost similar to the root. The transverse section of the rhizome is round. The rhizome structure consists of the epidermis, the cortex region, and the stele region (from the outside to the inside). The epidermis contains rectangular cells, arranged relatively regularly (Figure 6a). Under the epidermis is the suberized tissue, consisting of 5-7 cell layers (190-195 µm long), created by interlacing round or nearly round cells (dyed blue) (Figure 6b). The next layer is the thick-walled cortex, containing a multilayered hypodermis (5-6 layers, 32-35 µm long), with rectangular cells, arranged radially and concentrically (Figure 6c). The parenchymatous cells of the cortex are round (Figure 6d), irregularly arranged, and have small intercellular spaces between them. The endodermis has an obvious Casparian strip (Figure 6g). The polygonal pericycle (being adjacent to the endodermis) is a discontinuous cluster, surrounding the upper pole of the vascular bundles. There are scattered vascular bundles in the cortex and stele regions (150-160 µm in vertical diameter), distributed in the direction of the stele region. The number of vascular bundles in the stele region is higher than in the cortex region. Vascular bundles are surrounded by the sclerenchymatous conjunctive tissue, forming the vascular bundle sheath (Figure 6e). The sclereids (vascular bundle sheath) of vascular bundles in the cortex region are generally thicker than in the stele region. Vascular bundles are round or ovoid. Xylem vessels (Figure 6m), having about 1-6 scalariform perforation plates, are highly lignified. The phloem (Figure 6k) overlaps the xylem (Figure 6m). There are oil cells (Figure 6f) and starch grains scattered throughout the cortex and the stele regions.

Calcium oxalate is a common substance in the plant kingdom and appears in more than 215 plant families (McNair 1932). Plants produce various shapes and sizes of calcium oxalate crystals, with several proven functions, such as calcium regulation, plant protection, and heavy metal detoxification (Franceschi and Horner 1980). In the current study, an additional unique feature for *D. citrea* has been found, which is the absence of calcium oxalate in the roots and rhizomes. Calcium oxalate is commonly found in the roots of genera in the Zingiberaceae family, including the *Hedychium* (Gevú et al. 2014), *Curcuma* (Amel 2015), and *Kampferia* (Paopun 2020). The morphological features of calcium oxalate and its locations are conserved within specific taxa (Franceschi and Horner 1980). Moreover, changes in plant genomes can affect calcium oxalate's crystal nucleation, morphology, distribution, and number

(Nakata 2003). Thus, the lack of calcium oxalate crystals in the roots and rhizomes of *D. citrea* might be used to distinguish this species (or even the genus *Distichochlamys*) from other members in the Zingiberaceae family. However, this is the first time the anatomical structures of a *Distichochlamys* species have been studied. Therefore, further investigations on *Distichochlamys* anatomy need to be conducted to confirm the mentioned hypothesis.

In general, the micro-morphological characteristics of the roots and rhizomes of *D. citrea* are relatively similar. However, they also have some differences as shown in Figures 5 and 6. Roots have a wider cortex (composed of parenchyma cells, the narrow medullary region with many vascular bundles arranged discontinuously, xylem bundles interspersed with phloem, and a few cells located in the central medullary region). Compared to the roots, rhizomes have a wider medullary area and numerous vascular bundles (disorderly arranged and composed of phloem being above xylem).

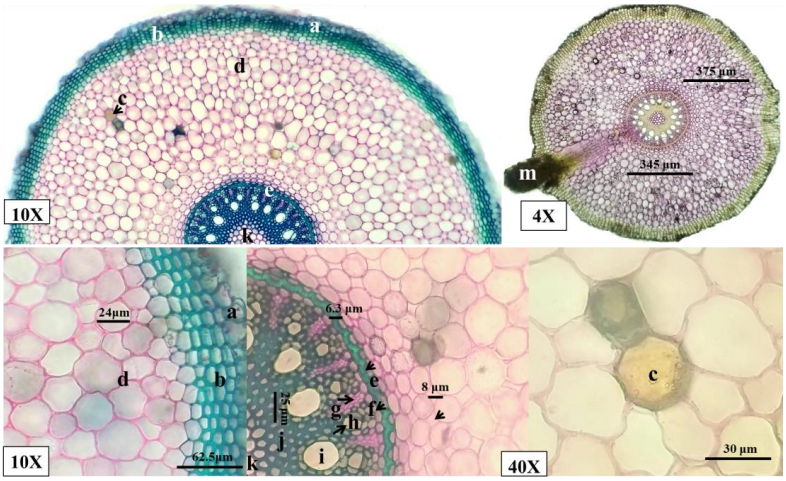

Figure 5. The features of *D. citrea*'s cross-sectioned root. (a) exodermis; (b) thick-walled cortex (suberized hypodermal cells); (c) oil cell; (d) cortex: (parenchymatous cells of the outer cortex and inner cortex); (e) "U" shape endodermis; (f) pericycle; (g) phloem; (h) protoxylem; (i) metaxylem); (j) sclerenchymatous conjunctive tissues; (k) parenchymatous pith; (m) lateral root formation.

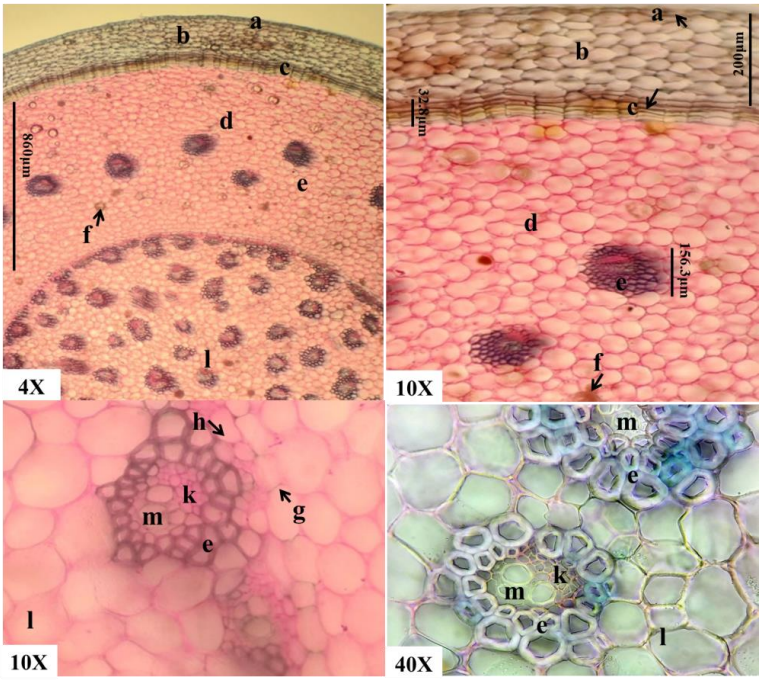

Figure 6. The features of *D. citrea*'s cross-sectioned rhizome: (a) epidermis; (b) exodermis (suberized tissue); (c) multilayered hypodermis; (d) the parenchymatous cells of cortex; (e) vascular bundle sheath; (f) oil cell; (g) casparian strips in endodermis; (h) pericycle; (k) phloem; (m) xylem; (l) parenchymatous pith

Powder

Rhizome powder

The dried root and rhizome powders are light-brown. The powders have fibers, a unique aroma, and a light spicy taste. Observing the powders under the microscope shows that they are characterized by the presence of almost components found in the fresh samples (Figure 8). Numerous fragments of thin-walled parenchyma consist of polygonal cells (Figures 8a and 8b). Starch granules are arranged in individual or clusters, which have ovoid or oval shapes (17-19 x 19-29 μm in diameter). The generally branched hilum of a starch granule is not in the middle of the granule and forms well-defined concentric lines (Figure 8c). The fragments of xylem vessels (forming spiral vessels (Figure 8d) and scalariform vessels (Figure 8e)) are commonly present in the observation field. Additionally, reddish-brown resin masses (Figure 8h), individual or bundles of thin-walled fibers (Figure 8n) are also found. The groups of sclereids composed of sclereid fibers (Figures 8l and 8m) and crystal fibers (Figures 8i-k) (with thick cell walls) are also observed. In the powder, there is also the presence of non-glandular trichomes (unicellular) (Figures 8q-s) and multicellular trichomes (Figure 8p)), which are intact or broken.

Leaf powder

The dried leaf powder is dark-green, odorless, and tasteless (Figure 9a). Observing the leaf powder under the microscope shows that it is characterized by the presence of different components, such as the polygonal fragments of epidermises (Figures 9b and 9c) (with thin cuticles), the paracytic stomata (Figure 9d), the fragments of parenchymatous cells (with thin walls) (Figures 9e and 9f), the abundant fragments of scalariform xylem vessel (with green chloroplast) (Figure 9g), the fragments of thick scalariform xylem vessel (Figure 9h), clusters of green chloroplasts (Figure 9i), the red-brown or black resin masses (Figures 9j-l), the elongated pericyclic fibers (with nearly rounded or sharp tips), and the lignified wood fibers (with thick walls) (Figures 9n and 9o). In general, most of the constituents found in fresh leaves were also found in the leaf powder. However, some components, such as upper epidermic, lower epidermic, and hypodermic cells were difficult to distinguish in leaf powder since we could not determine their locations.

Powder structures can be easily observed in fresh conditions. However, in the case of dry samples, tissues are deformed and become similar to one another regardless of species. Thus, powder analysis will help in differentiating the medicinal herbs since the unique micromorphological features of the examined species can be exposed and observed. Microscopic analyses of medicinal ingredients need to be combined with powder authentication to increase the accuracy of species identification (Aeri et al. 2020).

Since the rhizome is the valuable organ of plants in the family Zingiberaceae, only a few studies mention the examination of the leaf powders of these species. Particularly, only the leaf powders of *Alpinia calcarata*, *A. galanga*, and *Globba marantina* were analyzed (Mathew et al. 2014; Roy et al. 2016). *D. citrea* has red resin masses in the leaf powder which are not present in the mentioned species. Additionally, no aleurone grain, oil globule, and Si crystal were observed in Black Ginger's leaf powder as in *G. marantina* (Roy et al. 2016). *D. citrea* also does not have trichomes, observed in the leaf powders of *A. calcarata* and *A. galanga* (Mathew et al. 2014).

D. citrea has several unique rhizome powder characteristics. First, this species has multicellular trichomes which do not appear in other described members of Zingiberaceae, including *A. calcarata*, *A. galanga*, *Curcuma longa*, *C. caesia*, *G. marantina*, and *Z. officinale*. Moreover, there were no observed Si or calcium oxalate crystal in the rhizome powder of *D. citrea* (Paliwal et al. 2011; Wijayasiriwardena and Premakumara 2012; Mathew et al. 2014; Roy et al. 2016; Danapur and Venugopal 2019; Aye 2020). Oil droplets (which are present in *Z. officinale*) were also not detected in the rhizome powder of *D. citrea* (Aye 2020). The resin masses of *D. citrea* have the same color (red) as *C. longa* and *C. caesia* (Danapur and Venugopal 2019; Paliwal et al. 2022).

Molecular characters

The agarose gel electrophoresis revealed that the amplicons, produced by the ITS primers, had lengths of approximately 750 bp (Figure 10). After the Sanger sequencing and editing of the obtained sequence, the final amplicons' length was 647 bp.

BLAST-based comparisons between our sequenced amplicons and the reference sequences indicated that our PCR products were 96.54% similar (E-value = 0.0, query coverage = 97 %) to the ITS of *D. citrea* on Genbank (AF478744). Our sequence was then submitted to Genbank with the accession number MZ310840. The maximum likelihood dendrogram showed that ITS was suitable for identifying *D. citrea* though the identity between MZ310840 and AF478744 (shown by BLAST) was only 96.54%. The sequence of Bach Ma (MZ310840) clustered with other sequences of *D. citrea* from Genbank and this cluster was separated from other sequences of the Zingiberaceae family. Specifically, the distance between MZ310840 and the sequences of *D. citrea* was 0.019, which was smaller than that between MZ310840 and the sequences from other species. The closest ITS sequence to the *D. citrea* cluster was HM236130 (*D. rubrostriata*), with a distance of 0.039 (Figure 11).

Figure 7. Root and rhizome powders of *D. citrea*: (A) before sieving, (B) after sieving

The results demonstrated that ITS is reliable and efficient enough to identify *D. citrea*. This conclusion was in line with many authors using ITS to discriminate species in the family Zingiberaceae. Particularly, Vinitha et al. (2014) found that ITS was the marker revealing the highest interspecific distances (12-18.8 %) among 60 samples in 20 species of the family Zingiberaceae. Additionally, Labrooy et al. (2018) successfully identified seven *Kaempferia* species (Zingiberaceae) using ITS, with the BLAST identities between the authors' sequences and the reference sequences of 97 - 100 %. A high success rate of 96.97 % was also obtained when Tan et al. (2020) used ITS to identify 11 *Alpinia* species.

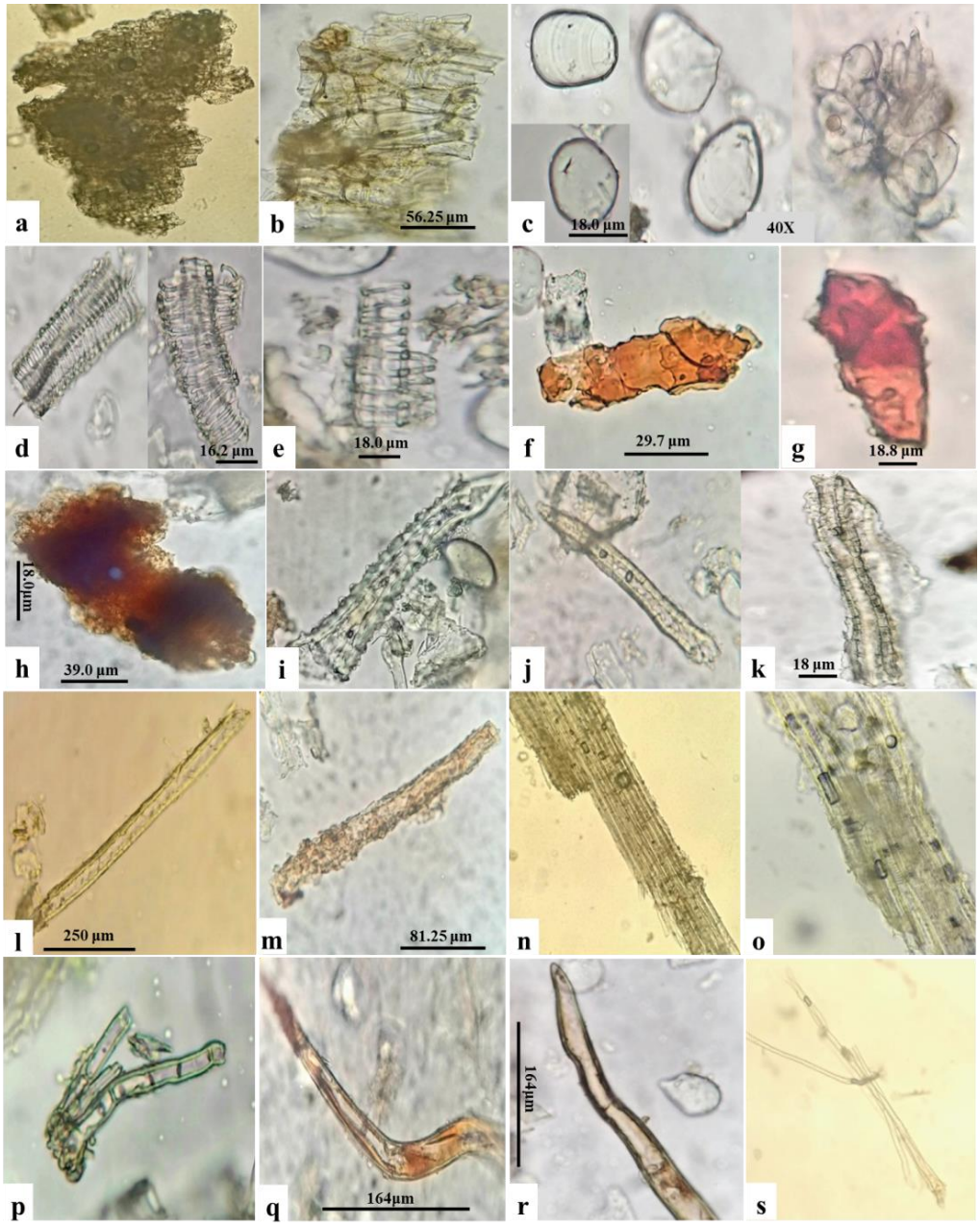

Figure 8. The features of root and rhizome powders of *D. citrea*: (a) parenchymatous cells; (b) epidermal cells; (c) starch granules; (d) spiral xylem vessel; (e) scalariform xylem vessel; (f, g) brown cork masses; (h) red-brown resin masses; (i, j, k) crystal fibers; (l, m) sclereid fibers; (n) bundle of fibers; (o) fragments of scalariform xylem vessel; (p) non-glandular multicellular trichomes; (q, r, s) non-glandular unicellular trichomes

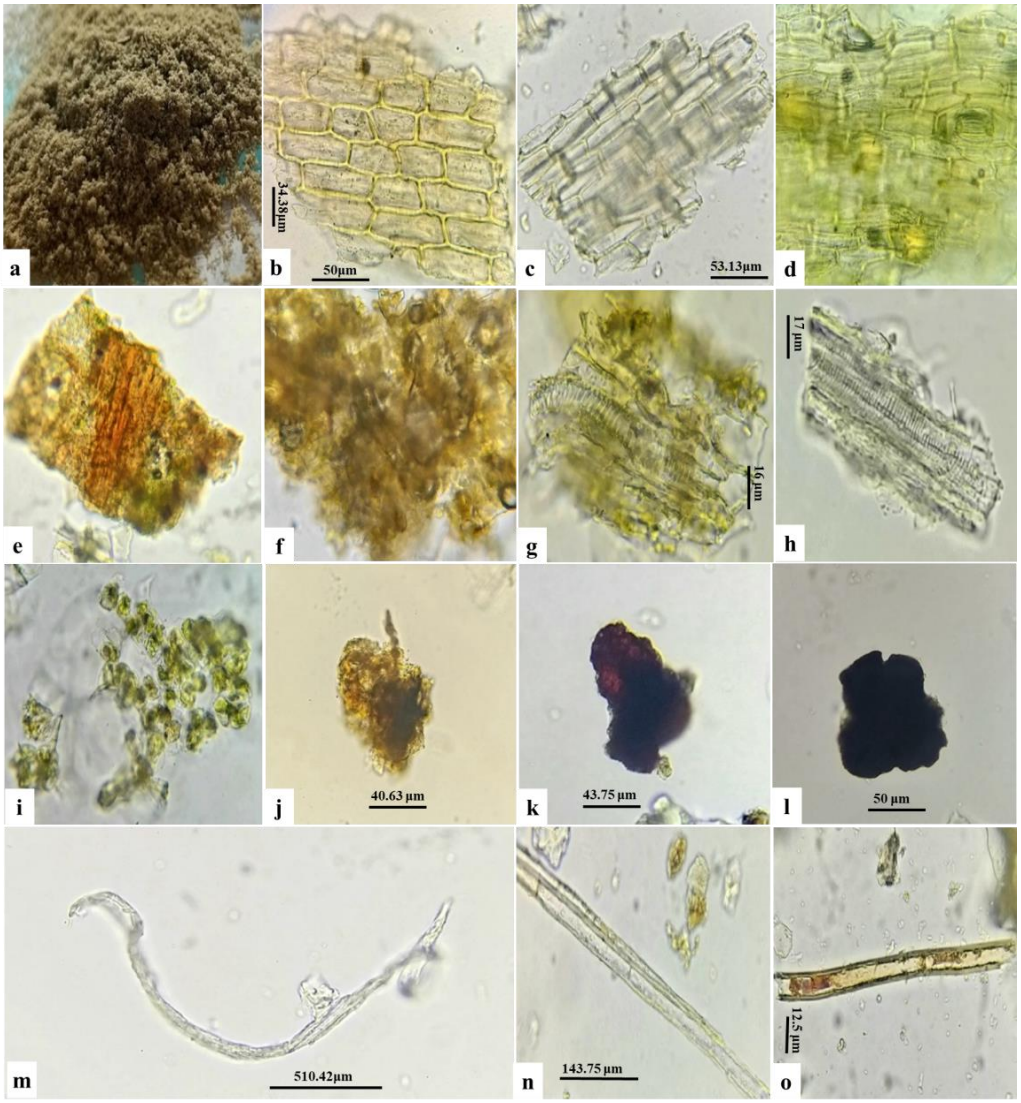

Figure 9. The features of dried leaf powder of *D. citrea*: (a) leaf powder; (b) surface view epidermis; (c) epidermal cells; (d) epidermis with stomata; (e, f) parenchymatous cells; (g) fragment of scalariform xylem vessel with green chloroplasts; (h) fragments of scalariform xylem vessel; (i) round-green of chloroplasts; (j, k, l) red-brown resin masses; (m) pericyclic fiber; (n, o) wood fibers

In addition to species in the family Zingiberaceae, many other species were also successfully identified by using ITS. Kress et al. (2005) claimed that ITS primers could amplify the DNA samples from five in eight genera of flowering plants and reveal the highest divergence rates in four genera (with a mean divergence rate of 2.8 %). Moreover, in the study on Amazonian trees, Gonzalez et al. (2009) showed that ITS was the second-best marker in the eight tested ones. Chen et al. (2010) also provided a high accuracy of 92.7 % obtained by using ITS to identify 4800 species. In the three mentioned studies, amplification failures were observed when ITS primers were used in PCR. However, they always showed high interspecific variances when the amplifications were successful. In our present study, no PCR failure was detected and the universal ITS primers could amplify *D. citrea* DNA samples. Thus, universal ITS primers can be conveniently used for *D. citrea* identification in the future.

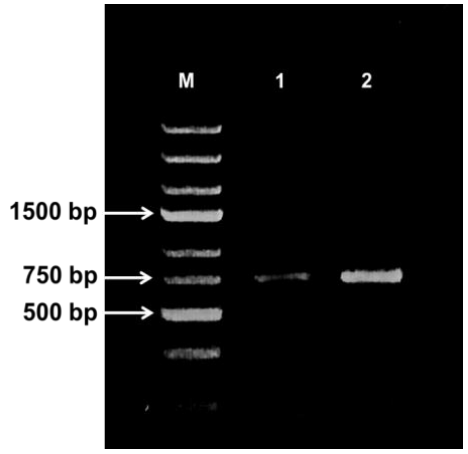

Figure 10. PCR products are generated by ITS1 and ITS4 primers. ("1" and "2" are two samples with the most obvious bands and "M" is the DNA ladder)

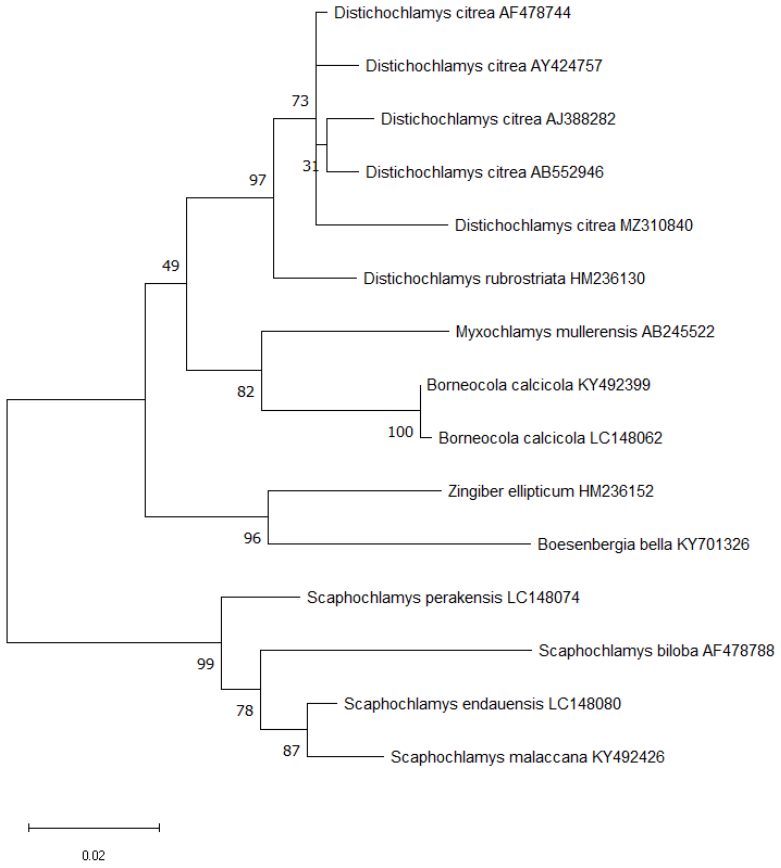

Figure 11. Maximum likelihood dendrogram of 15 ITS sequences. The ITS sequence of *D. citrea* from Bach Ma formed a cluster with the ITS sequences of the same species (AF478744, AY424757, AJ388282, and AB552946), separating from other species in the Zingiberaceae family. The numbers on the branches are bootstrap values in a percentage of 1000 replications

ACKNOWLEDGEMENTS

The authors thank the partial facility support of the Faculty of Traditional Medicine, University of Medicine and Pharmacy at Ho Chi Minh City for the identification of anatomical characteristics of *D. citrea*. Nguyen Thi Ai Nhung acknowledges the partial support of Hue University under the Core Research Program, Grant No. NCM.DHH.2020.04.

REFERENCES

Aeri V, Anantha Narayana DB, Singh D. 2020. Chapter 1 - Introduction to powder microscopy. In: Aeri V, Anantha Narayana DB, Singh D (eds). Powdered Crude Drug Microscopy of Leaves and Barks. Elsevier, United States. DOI: 10.1016/B978-0-12-818092-1.00001-4.

Alhousari F, Greger M. 2018. Silicon and mechanisms of plant resistance to insect pests. Plants 7 (2): 33. DOI: 10.3390/plants7020033.

Amel B. 2015. Microscopic analysis of *Curcuma longa* L. using multivariate test. Intl J Pharmacol 2 (4): 173-177. DOI: 10.13040/IJPSR.0975-8232.IJP.2(4).173-77.

Aye YY. 2020. Microscopical Characters, Phytochemical and FTIR Studies on Rhizome of *Zingiber officinale* Rosc. (Gyin). [Dissertation]. University of Mandalay Res J 11: 10-20.

Carnesecchi S, Bras-Gonçalves R, Bradaia A, Zeisel M, Gossé F, Poupon M-F, Raul F. 2004. Geraniol, a component of plant essential oils, modulates DNA synthesis and potentiates 5-fluorouracil efficacy on human colon tumor xenografts. Cancer Lett 215 (1): 53-59. DOI: 10.1016/j.canlet.2004.06.019.

Chen S, Yao H, Han J, Liu C, Song J, Shi L, Zhu Y, Ma X, Gao T, Pang X. 2010. Validation of the ITS2 region as a novel DNA barcode for identifying medicinal plant species. PloS One 5: e8613. DOI: 10.1371/journal.pone.0008613.

Cheng T, Xu C, Lei L, Li C, Zhang Y, Zhou S. 2016. Barcoding the kingdom Plantae: new PCR primers for ITS regions of plants with improved universality and specificity. Mol Ecol Resour 16 (1): 138-149. DOI: 10.1111/1755-0998.12438.

Conklin KY, Kurihara A, Sherwood AR. 2009. A molecular method for identification of the morphologically plastic invasive algal genera *Eucheuma* and *Kappaphycus* (Rhodophyta, Gigartinales) in Hawaii. J Appl Phycol 21 (6): 691-699. DOI: 10.1007/s10811-009-9404-2.

Danapur V, Venugopal RB. 2019. Pharmacognostic Studies on *Curcuma longa*. Intl J Pharmacogn Chinese Med 3: 000163. DOI: 10.23880/ipcm-16000163.

Franceschi VR, Horner HT. 1980. Calcium oxalate crystals in plants. Bot Rev 46 (4): 361-427. DOI: 10.1007/BF02860532.

Gevú KV, Da Cunha M, Barros CF, Pereira SM, Lima HRP. 2014. Structural analysis of subterranean organs in Zingiberaceae. Plant Syst Evol 300 (5): 1089-1098. DOI: 10.1007/s00606-013-0947-y.

Gonzalez MA, Baraloto C, Engel J, Mori SA, Pétronelli P, Riéra B, Roger A, Thébaud C, Chave J. 2009. Identification of Amazonian trees with DNA barcodes. PLoS One 4: e7483. DOI: 10.1371/journal.pone.0007483

Greger M, Landberg T, Vaculík M. 2018. Silicon influences soil availability and accumulation of mineral nutrients in various plant species. Plants 7 (2): 41. DOI: 10.3390/plants7020041.

Hebert PDN, Ratnasingham S, De Waard JR. 2003. Barcoding animal life: cytochrome c oxidase subunit 1 divergences among closely related species. Proc R Soc Lond B Biol Sci 270 (1): S96-S99. DOI: 10.1098/rsbl.2003.0025.

Hoang HTN, Dinh TTT, Pham TV, Le HBT, Ho DV. 2020. Chemical composition and acetylcholinesterase inhibitory activity of essential oil from rhizomes of *Distichochlamys benenica*. HU JOS 129 (1D): 43-49. DOI: 10.26459/hueunijns.v129i1D.5804.

Hollingsworth PM, Graham SW, Little DP. 2011. Choosing and using a plant DNA barcode. PloS one 6: e19254. DOI: 10.1371/journal.pone.0019254.

Huong LT, Chau DTM, Hung NV, Dai DN, Ogunwande IA. 2017. Volatile constituents of *Distichochlamys citrea* MF Newman and *Distichochlamys orlowii* K. Larsen MF Newman (Zingiberaceae) from Vietnam. J Med Plant Res 11 (9): 188-193. DOI: 10.5897/JMPR2016.6337.

Kamatou GPP, Viljoen AM. 2008. Linalool-A review of a biologically active compound of commercial importance. Nat Prod Commun 3 (7): 1183-1192. DOI: 10.1177/1934578X0800300727.

Khaleel C, Tabanca N, Buchbauer G. 2018. α-Terpineol, a natural monoterpene: A review of its biological properties. Open Chem 16 (1): 349-361. DOI: 10.1515/chem-2018-0040.

Khanuja SPS, Shasany AK, Darokar MP, Kumar S. 1999. Rapid isolation of DNA from dry and fresh samples of plants producing large amounts of secondary metabolites and essential oils. Plant Mol Biol Rep 17 (1): 74-74. DOI: 10.1023/A:1007528101452.

Kress WJ, Erickson DL. 2007. A two-locus global DNA barcode for land plants: the coding *rbcL* gene complements the non-coding *trnH-psbA* spacer region. PLoS One 2: e508. DOI: 10.1371/journal.pone.0000508.

Kress WJ, Prince LM, Williams KJ. 2002. The phylogeny and a new classification of the gingers (Zingiberaceae): evidence from molecular data. Am J Bot 89 (10): 1682-1696. DOI: 10.3732/ajb.89.10.1682.

Kress WJ, Wurdack KJ, Zimmer EA, Weigt LA, Janzen DH. 2005. Use of DNA barcodes to identify flowering plants. PNAS 102 (23): 8369-8374. DOI: 10.1073/pnas.0503123102.

Labrooy CD, Abdullah TL, Stanslas J. 2018. Identification of ethnomedicinally important *Kaempferia* L. (Zingiberaceae) species based on morphological traits and suitable DNA region. Cur Plant Biol 14: 50-55. DOI: 10.1016/j.cpb.2018.09.004.

Larsen K, Newman MF. 2001. A new species of *Distichochlamys* from Vietnam and some observations on generic limits in *Hedychieae* (Zingiberaceae). Nat Hist Bull Siam Soc 49: 77-80. DOI: 10.1663/0007-196X(2003)055[0205:DRZANS]2.0.CO;2.

Li DZ, Liu JQ, Chen ZD, Wang H, Ge XJ, Zhou SL, Gao LM, Fu CX, Chen SL. 2011. Plant DNA barcoding in China. J Syst E 49: 165-168. DOI: 10.1111/j.1759-6831.2011.00137.x.

Li J, Lin X, Tang G, Li R, Wang D, Ji S. 2019. Pharmacognostical study of *Desmodium caudatum*. An Acad Bras Cienc 91 (2): e20180637. DOI: 10.1590/0001-3765201920180637.

Liu H, Specht CD, Zhao T, Liao J. 2020. Morphological anatomy of leaf and rhizome in *Zingiber officinale* Roscoe, with emphasis on secretory structures. Hort Sci 55 (2): 204-207. DOI: 10.21273/HORTSCI14555-19.

Mathew S, Britto SJ, Thomas S. 2014. Comparative powder microscopical screening of the rhizome and leaf of *Alpinia calcarata* and *Alpinia galanga*. Intl J Pharm Sci Res 5 (4): 1449. DOI: 10.13040/IJPSR.0975-8232.5(4).1449-53

McNair JB. 1932. The interrelation between substances in plants: essential oils and resins, cyanogen and oxalate. Am J Bot 19 (3): 255-272. DOI: 10.2307/2436337.

Ministry of Health. 2017. Vietnamese Pharmacopoeia V: Medical Publishing House. Hanoi, Vietnam.

Mood JD, Veldkamp JF, Mandáková T, Prince LM, deBoer HJ. 2019. Three new species of *Boesenbergia* (Zingiberaceae) from Thailand and Lao P.D.R. Gard Bull Singap 71: 477-498. DOI: 10.26492/gbs71(2).2019-15.

Moteki H, Hibasami H, Yamada Y, Katsuzaki H, Imai K, Komiya T. 2002. Specific induction of apoptosis by 1,8-cineole in two human leukemia cell lines, but not a in human stomach cancer cell line. Oncol Rep 9 (4): 757-760. DOI: 10.3892/or.9.4.757.

Nakata PA. 2003. Advances in our understanding of calcium oxalate crystal formation and function in plants. Plant Sci 164 (6): 901-909. DOI: 10.1016/S0168-9452(03)00120-1.

Newman MF. 1995. *Distichochlamys*, a new genus from Vietnam. Edinb J Bot 52 (1): 65-69. DOI: 10.1017/S096042860000192X.

Ngamriabsakul C, Newman MF, Cronk QCB. 2003. The phylogeny of tribe Zingibereae (Zingiberaceae) based on *its* (nrDNA) and *trnl-f* (cpDNA) sequences. Edinb J Bot 60 (3): 483-507. DOI: 10.1017/S0960428603000362.

Nguyen QB, Leong-Škorničková J. 2012. *Distichochlamys benenica* (Zingiberaceae), a new species from Vietnam. Gard Bull (Singap) 64: 195-200.

Ooi IH. 2018. Taxonomy, Phylogenetic Analyses and Pollination Biology of *Scaphochlamys* (Zingiberaceae) of Borneo. [Dissertation]. Universiti Malaysia Sarawak (UNIMAS). [Malaysian]

Packer L, Gibbs J, Sheffield C, Hanner R. 2009. DNA barcoding and the mediocrity of morphology. Mol Ecol Resour 9: 42-50. DOI: 10.1111/j.1755-0998.2009.02631.x.

Paliwal P, Pancholi SS, Patel RK. 2011. Pharmacognostic parameters for evaluation of the rhizomes of *Curcuma caesia*. J Adv Pharm Technol 2 (1): 56. DOI: 10.4103/2231-4040.79811.

Paopun Y. 2020. Calcium oxalate crystals and leaf anatomical characteristics of *Kaempferia galanga* L. J Microsc Soc Thail 33 (1): 28-33. DOI: 10.14456/microsc-microanal-res.2020.7.

Quintans-Júnior LJ, Guimarães AG, Santana MTd, Araújo BES, Moreira FV, Bonjardim LR, Araújo AAS, Siqueira JS, Antoniolli ÂR, Botelho MA. 2011. Citral reduces nociceptive and inflammatory response in rodents. Rev Bras Farmacogn 21 (3): 497-502. DOI: 10.1590/S0102-695X2011005000065.

Rehse T, Kress WJ. 2003. *Distichochlamys rubrostriata* (Zingiberaceae), a new species from northern Vietnam. Brittonia 55 (3): 205-208. DOI: 10.1663/0007-196X(2003)055[0205:DRZANS]2.0.CO;2

Roy S, Acharya RN, Harisha CR, Shukla VJ. 2016. Macro, microscopic and preliminary analytical evaluation of root and leaf of *Globba marantina* Linn.- An extrapharmacopoeial drug of Ayurveda. Indian J Pharm Sci 78 (4): 469-478. DOI: 10.4172/pharmaceutical-sciences.1000141.

Rudall PJ, Chen ED, Cullen E. 2017. Evolution and development of monocot stomata. Am J Bot 104 (8): 1122-1141. DOI: 10.3732/ajb.1700086.

Sam YY, Takano A, Ibrahim H, Záveská E, Aziz F. 2016. Borneocola (Zingiberaceae), a new genus from Borneo. PhytoKeys 75: 31-55. DOI: 10.3897/phytokeys.75.9837

Searle RJ, Hedderson TA. 2000. A preliminary phylogeny of the Hedychieae tribe (Zingiberaceae) based on ITS sequences of the nuclear rRNA cistron. In: Wilson K, Morrin D (eds). Monocotyledons: Systematics and Evolution. CSIRO Publishing, Clayton, Australia.

Szczepaniak M, Cieslak E, Bednarek PT. 2002. Morphological and AFLP variation of *Elymus repens* (L.) Gould (Poaceae). Cell Mol Biol Lett 7 (2A): 547-558.

Takano A, Nagamasu H. 2007. *Myxochlamys* (Zingiberaceae), a new genus from Borneo. Acta Phytotaxonomica et Geobotanica 58 (1): 19-32.

Tan WH, Chai LC, Chin CF. 2020. Efficacy of DNA barcode internal transcribed spacer 2 (ITS 2) in phylogenetic study of Alpinia species from Peninsular Malaysia. Physiol Mol Biol Plants 26 (9): 1889-1896. DOI: 10.1007/s12298-020-00868-1.

Techen N, Parveen I, Pan Z, Khan IA. 2014. DNA barcoding of medicinal plant material for identification. Curr Opin Biotechnol 25: 103-110. DOI: 10.1016/j.copbio.2013.09.010.

Ty PV, Hoai NT, Khan NV, Duc HV. 2017. Chemical composition of the essential oils of *Distichochlamys citrea* leaves collected from central Vietnam. Vietnam J Chem 55: 358-362.

Uma E, Muthukumar T. 2014. Comparative root morphological anatomy of Zingiberaceae. Syst Biodivers 12 (2): 195-209. DOI: 10.1080/14772000.2014.894593.

Vinitha MR, Kumar US, Aishwarya K, Sabu M, Thomas G. 2014. Prospects for discriminating Zingiberaceae species in India using DNA barcodes. J Integr. Plant Biol 56 (8): 760-773. DOI: 10.1111/jipb.12189.

Wijayasiriwardena C, Premakumara S. 2012. Comparative powder microscopy of *Alpinia calcarata* Roscoe and *Alpinia galanga* (Linn.) Willd. Ayu 33 (3): 441. DOI: 10.4103/0974-8520.108863.

Yan GC, Nikolic M, Ye MJ, Xiao ZX, Liang YC. 2018. Silicon acquisition and accumulation in plant and its significance for agriculture. J Integr Agric 17 (10): 2138-2150. DOI: 10.1016/S2095-3119(18)62037-4.

Yao H, Song J, Liu C, Luo K, Han J, Li Y, Pang X, Xu H, Zhu Y, Xiao P. 2010. Use of *ITS2* region as the universal DNA barcode for plants and animals. PloS One 5: e13102. DOI: 10.1371/journal.pone.0013102.

Zahara M. Year. Identification of morphological and stomatal characteristics of Zingiberaceae as medicinal plants in Banda Aceh, Indonesia. In: Samadi, Yunita D, Goritno AD (eds). IOP Conf Ser: Earth Environ Sci. The 1st International Conference on Agriculture and Bioindustry, Banda Aceh, Indonesia, 24-26 October 2019. DOI: 10.1088/1755-1315/425/1/012046. [Indonesian]

Zheng ML, Xia YM. 2010. A Investigation on The Phylogeny of Tribe Zingibereae (Zingiberaceae) Based on nrDNA ITS and cpDNA matK Sequence Data. [Dissertation]. Yunnan University. [Chinese]